



RESEARCH ARTICLE OPEN ACCESS

A Smart Camera With Integrated Deep Learning Processing for Disease Detection in Open Field Crops of Grape, Apple, and Carrot

Gerrit Polder¹  | Pieter M. Blok¹  | Tim van Daalen¹ | Joseph Peller¹ | Nikos Mylonas²

¹Wageningen Plant Research, Wageningen University & Research, Wageningen, The Netherlands | ²Agricultural Engineering, Agricultural University of Athens, Athens, Greece

Correspondence: Gerrit Polder (gerrit.polder@wur.nl)

Received: 30 August 2022 | **Revised:** 30 September 2024 | **Accepted:** 12 December 2024

Funding: This paper is supported by European Union's Horizon 2020 research and innovation programme under grant agreement No 773718, project OPTIMA (Optimised Pest Integrated Management to precisely detect and control plant diseases in perennial crops and open-field vegetables).

Keywords: convolutional neural networks | integrated pest management | IPM | machine vision | object detection | open set recognition/classification | smart sprayer

ABSTRACT

Downy mildew (*Plasmopara*), apple scab (*Venturia inaequalis*), and *Alternaria* leaf blight are endemic diseases that affect crops worldwide. The diseases can cause severe losses in grapes, apples and carrots when not detected and treated in an early stage. The European Union Horizon 2020 OPTIMA project aimed to improve disease detection in the open field with an automated detection system as part of an integrated pest management (IPM) system. In this research, we investigated the automated detection of downy mildew in grape, apple scab in apple and *Alternaria* leaf blight in carrot, using a deep convolutional neural network (CNN) on RGB color images. Detections from the CNN served as input to a Decision Support System (DSS), to precisely locate and quantify the disease, so that appropriate and timely application of plant protection products could be recommended. The focus of our study was on a smart camera implementation with integrated deep-learning processing in real-field conditions. The question was whether the deep learning model, when trained on images of disease symptoms recorded in conditioned circumstances, can also perform on images of disease symptoms recorded in field conditions. This type of evaluation is called open-set evaluation, and so far it has received little attention in plant disease detection research. Therefore, the goal of our research was to evaluate the performance of a deep learning model in an open-set evaluation scenario in commercial vineyards, orchards, and open fields. The model's performance in the open-set scenario was compared to its performance in the closed-set scenario, which involved evaluating the trained model on images similar to those used for model training. Our results showed that the model's performance in the closed-set scenario with *F1* scores of 66.3% (downy mildew), 45.1% (apple scab), and 42.1% (*Alternaria*) was notably better than in the open-set scenario, with *F1* scores of 34.8% (downy mildew), 5.5% (apple scab) and 4.2% (*Alternaria*). Uniform Manifold Approximation and Projection (UMAP) analysis proved the significant difference between the open-set and closed-set data sets. Our result should encourage other researchers to carry out similar open-set evaluations to get realistic impressions of their model's performance under field conditions. A subset of our image data set has been made publicly available at <https://doi.org/10.5281/zenodo.6778647>.

This is an open access article under the terms of the [Creative Commons Attribution](https://creativecommons.org/licenses/by/4.0/) License, which permits use, distribution and reproduction in any medium, provided the original work is properly cited.

© 2025 The Author(s). *Journal of Field Robotics* published by Wiley Periodicals LLC.

1 | Introduction

The global population is expected to reach 9.8 billion by 2050 (United Nations 2015). To feed this population, agricultural production will need to increase heavily over current levels, with an efficient use of resources. Furthermore, the total crop yield reduction caused by all crop pests and diseases reaches 40% (Oerke et al. 1994), causing the global food security to be undermined (Chandler et al. 2011). The use of traditional plant protection products to protect crops against pests and diseases unfortunately has negative impacts on the environment, biodiversity, and human health and should therefore be largely reduced. Ways to make crop protection more sustainable are required and integrated pest management (IPM) is promoted as the best way forward making a difference in this effort. IPM emphasizes the growth of a healthy crop with the least possible disruption to agro-ecosystems (Lamichhane et al. 2016). In IPM systems approach that combines different crop protection practices is implemented. It discourages the development of populations of harmful organisms and keeps the use of plant protection products to levels that are economically and ecologically justified, resulting in reduction or minimization of risks to human health and the environment. The EU Horizon 2020 OPTIMA project aimed to develop an advanced IPM framework that consist of 4 main pillars (Prediction, Detection, Selection and Application) (Balafoutis et al. 2019). The OPTIMA project will focus on three plant diseases that require large quantities of fungicides to be applied in numerous spraying applications. These plant diseases are downy mildew (*Plasmopara viticola*) in grapes, apple scab (*Venturia inaequalis*) in apples, and *Alternaria* leaf blight in carrot. All three diseases are endemic diseases that affect fruits and vegetables across the world. The diseases can cause severe losses in grapes, apples and carrots when not detected and treated in an early stage. Treatment can be done by spraying either copper sulfates or fungicides onto the crop before the fungi have sporulated (Ash 2000; Vaillancourt and Hartman 2000). However, excessive spraying has led to a rise in disease resistance and has a negative impact on the environment (Wightwick et al. 2012). Due to the large field sizes, the visual inspection of each leaf is too labor intensive, and instead machine vision could be useful. As part of the OPTIMA project a plant disease detection system is developed (Polder et al. 2021), based on machine vision using RGB color and spectral cameras (Peller et al. 2021). The detection system involves the precise localization and quantification of the infections. Predictive computer models implemented in a Decision Support System (DSS) use the disease detection to improve the disease pressure estimation to treat the diseases timely and precisely. Combined with improved spraying technology (Grella et al. 2022; Zwervaegher et al. 2022) and biological plant protection products (Natal-da Luz et al. 2019) a novel environmentally friendly IPM framework is developed.

1.1 | Related Work

Automatic plant disease detection using traditional image processing techniques has been explored for many years (Lindow 1983). Due to the nature of machine vision cameras with sensitivity that mimics the human eye, a lot of work has been done on automatic detection of visible symptoms (Garcia

and Barbedo 2013). Kole, Ghosh, and Mitra (2014) presents a technique for detection of downy mildew disease in grape leaves based on fuzzy importance factor. The proposed technique uses digital image processing operations and fuzzy set theory concept with an 87.09% success rate. Using the advanced symptoms of apple scab on fruits, Agarwal, Sarkar, and Dubey (2019) has been able to use traditional machine vision to correctly identify diseased fruits. A system based on texture features an a Random Forest classifier achieved best classification accuracy of 86%, while using images of grapes leaves with complex background which are captured under an uncontrolled environment (Sandika et al. 2016). Waghmare et al. (2016) proposed a fractal based texture feature method combined with a multi class Support Vector Machine classifier to detect downy mildew & black rot in grapes with an accuracy of 96.6%. Recently, also spectral imaging has been applied for disease detection using a large number of smaller wavelength bands over a range larger than the visible spectrum (Mahlein et al. 2018; Mishra, Polder, and Vilfan 2020).

Recently, deep learning has evolved as a new research direction in the field of machine learning and has been widely applied to various tasks such as computer vision, image classification, object detection, video data analysis, speech recognition, and multimedia retrieval, achieving excellent results (LeCun, Bengio, and Hinton 2015). Also in the field of agriculture and specifically plant disease detection a lot of research has been done. Kamilaris and Prenafeta-Boldú (2018) performed a survey of 40 research efforts that employ deep learning techniques, applied to various agricultural and food production challenges. Comparison with traditional machine learning methods indicated that deep learning provides high accuracy, outperforming existing commonly used feature-engineered image processing techniques. From the 40 papers of this review, only 3 were on disease detection (Amara, Bouaziz, and Alergawy 2017; Mohanty, Hughes, and Salathé 2016; Singh et al. 2016) which indicates that disease detection is a challenging task, compared to other applications. Dhaka et al. (2021) performed a survey on the prediction of plant leaf diseases using Convolutional Neural Networks (CNNs), which are image-based deep learning models (LeCun, Bengio, and Hinton 2015). The research of Dhaka et al. (2021) focused on the use and size of the data sets, image pre-processing techniques, CNN architectures, CNN frameworks, performance metrics, and experimental results of different models. The authors concluded that existing research focuses on disease identification and classification at the image level, but currently lack localization of the diseased regions in the image. Ahmad, Saraswat, and El Gamal (2023) presents a comprehensive overview of 70 studies on deep learning applications and the trends associated with their use for disease diagnosis and management in agriculture, focusing on providing a detailed assessment for developing deep learning-based tools in the form of seven key questions, helping to address existing research gaps. Liu et al. (2018) propose an accurate identifying approach for apple leaf diseases based on CNNs using an initial data set of 1053 images of cut apple leaves captured on a gray background.

A lot of research has been done utilizing the openly available PlantVillage data set (Hughes and Salathé 2015), which consists of 54,306 images of 14 crop species with 26 diseases (or healthy)

(Mohanty, Hughes, and Salathé 2016; Too et al. 2019; Pradhan, Kumar, and Mohan 2022). For the crops of interest to the OPTIMA project, only apple leaves with scab and healthy are represented in PlantVillage. Besides healthy grape images and some other diseases, no downy mildew-infected grape leaf images are available in PlantVillage and carrot is not present in PlantVillage.

Due to the lack of grape downy mildew in public data sets, limited work is done on its detection. Zhu et al. (2020) proposed an automatic detection method for five grape leaf diseases, including downy mildew, based on image analysis and back-propagation neural networks, yielding a 90% classification accuracy for downy mildew. Grapevine yellow disease was detected in a data set of 322 images and six diseases, including downy mildew, using a linear support vector machine (SVM) that classified features from a pre-trained CNN with 95.23% accuracy (Ampatzidis et al. 2020). Liu et al. (2020) developed and trained a novel CNN-based model, from scratch. This model had an overall accuracy of 97.22% on a total of 7669 images of grape leaves from which 910 showed downy mildew symptoms. The lack of sufficient annotated images can also be solved by using data augmentation using generative adversarial networks (Chen and Wu 2022).

For detection of apple scab more work can be found in the literature, initiated by the existence of scab infected and healthy leaf images in PlantVillage. Furthermore, Kaggle provides a public data set built for the Plant Pathology Challenge for the CVPR 2020 FGVC7 workshop (Thapa et al. 2020). This data set consists of 3651 high-quality annotated RGB images showing symptoms of cedar apple rust and apple scab, as well as leaves displaying complex disease symptoms and healthy apple leaves. Ayaz et al. (2021) investigated different CNN applications to apple disease classification using deep generative images to obtain higher accuracy than existing models (i.e., ResNet, SqueezeNet, and MiniVGNet). They are using a subset of the Kaggle data set of 319 images, from which 80 healthy and 79 apple scab. Yan et al. (2020) proposed an improved model based on VGG16 to identify apple leaf diseases. The experimental results show that the overall accuracy of apple leaf classification based on the proposed model can reach 99%. Compared with the classical VGG16, the recognition accuracy is improved by 6.3%. The data set in this work is extracted from the “2008 ‘AI Challenger’ Global Challenge” and includes 2446 pictures of cut apple leaves imaged on a uniform background, where 1340 of them are healthy and 411 are scab. Li, Jing, and Shi (2022) proposed an apple disease recognition method based on modified CNNs, using the Inception module, global average pooling, and a modified softmax classifier to improve the recognition performance. A series of experiments were conducted on the Kaggle and YangLing apple disease image data sets. The Yangling data set contains 450 diseased leaf images of three kinds of disease: *Alternaria* leaf spot, Mosaic, and Rust. Leaves were picked in fields and imaged in the laboratory, with one leaf per image, as flat as possible on a simple gray background. Detection accuracy is good on both data sets, but field application is a challenging task, since contrary to this experiment field images will contain a lot of background and noise, submerging the disease spot features in the images, resulting in degraded disease detection and recognition. Many other papers on scab

detection also use images from Kaggle or PlantVillage (Subetha, Khilar, and Christo 2021; Khan et al. 2020; Darshan 2020; Bansal, Kumar, and Kumar 2021; Kodors et al. 2021). In contrast, Singh et al. (2022) acquired a database of 50,000 images of leaves from apple farms of Himachal Pradesh (H.P) and Uttarakhnad (India). In this research work, a CNN with 19 convolutional layers has been proposed for effective and accurate classification of *Marsonina Coronaria* and apple scab from apple leaves.

Presumably due to the lack of *Alternaria* leaf blight infected carrot leaf images in public data sets, no research could be found on imaging-based disease detection methods with traditional or deep learning based machine learning methods.

Although many of the papers mentioned above show promising results on images from public data repositories, care needs to be taken when interpreting the results. Recently, it has been demonstrated that images in the PlantVillage data set suffer from background and capture bias. A model trained on only eight background pixels achieved 49.0% accuracy, well above the random guessing accuracy of 2.6% (Noyan 2022). Performance of trained networks based on this data when implemented in real-time field detection systems will certainly drop notably.

1.2 | Goal of This Paper

Although that significant advances have been made in the field of image-based plant disease detection, it must be acknowledged that in previous studies the disease detection was performed on fixed-sized data sets with limited variation. Besides that, in previous studies, the evaluation was done in a so-called closed-set evaluation scenario. A closed-set evaluation means that the images used during model testing are similar to the images used during model training (Sünderhauf et al. 2018). A risk when testing in a closed set evaluation scenario, is that it is not known whether the trained model can perform on new types of images taken with different hardware under different field conditions. Therefore, this study examines whether a model trained on images of disease symptoms recorded in conditioned circumstances can also perform on images of disease symptoms recorded in field conditions. This type of evaluation is called open-set evaluation. To date, open-set evaluation has received little attention in plant disease detection research. The goal of this research was to evaluate the plant disease detection performance of a deep learning model in a closed-set and open-set evaluation scenario in commercial orchards, vineyards, and open fields. Our research focused on using a smart camera system for detecting downy mildew in grapes, apple scab in apples, and *Alternaria* leaf blight in carrots. The smart camera system consisted of an RGB camera with an embedded processing unit that could directly process an image after it was acquired. In our research, the smart camera was equipped with a deep learning object detection model. Besides the smart camera, the integrated system was equipped with a Global Navigation Satellite System (GNSS) for localization and a cloud connection to a Decision Support System (DSS) for follow-up actions (such as spot-specific spraying). In summary, our paper contributes the following:

1. A description of the development of a smart camera-based plant disease detection system on leaf-level, with GNSS localization and cloud connection to a decision support system.
2. A performance evaluation of this integrated smart camera system in closed-set and open-set evaluation scenarios in three realistic food production environments, including an outline of the challenges that this system faces in such complex and challenging environments.
3. The public release of three subsets of our data sets (including annotations): <https://doi.org/10.5281/zenodo.6778647>.

This paper is organized as follows: the overall system, hardware and software components of the smart camera system are described in Section 2. Section 3 describes the setup for the field evaluation. Section 4 describes the performance of the system in the commercial vineyards, orchards, and fields. Section 6 concludes this work with the research conclusions and recommendations for future research.

2 | System Architecture

2.1 | Overall Smart Sprayer System Overview

The smart camera system was part of a larger IPM approach, as shown in Figure 1. In phase one, images are acquired and analyzed by the smart camera. The outputs are sent to the DSS. In phase two, the DSS creates a prescription map for the smart sprayer, based on the outputs of the smart camera system, and the historical and meteorological data. In phase three, the prescription map is uploaded onto the on-board computer of the smart sprayer, so that the spraying action can be executed. In IPM, variable-rate sprayers, which adjust the application rates using flow controllers based on information from real-time or sensor-guided canopy detection systems, or disease detection systems either using a DSS or in real time as described in this paper, are able to precisely spray only spots where needed (Grella et al. 2022).

The innovative agriculture smart sprayer integrates advanced vision systems with precise actuation mechanisms to optimize

pesticide application. Utilizing either CANBUS messages or custom serial messages, this system facilitates seamless data exchange between the sprayer's electronic control unit (ECU) and the embedded processing unit of the vision system. Before each spraying session, prescription maps, detailing areas of infestation, are uploaded to the ECU. As the spraying operation commences, real-time GPS data is harnessed to pinpoint the sprayer's location relative to these infestation zones. Whenever the sprayer's GPS coordinates align with these predefined infestation areas, the sprayer ECU administers the maximum prescribed rate. This targeted application is achieved by sending actuation commands ranging from 0% to 100% duty cycle to the pulse width modulation (PWM) system for grapevines and electric solenoid valves for apples. When the sprayer traverses outside infestation zones, different application strategies are selected, depending on the epidemiological severity and agronomic conditions, for example spraying 80% of the maximum application outside the infestation zones, or even shutting off the nozzles outside the diseased parts. Crucially, the final pesticide dosage rate is not solely based on infestation data; it is also influenced by ultrasound real-time foliage estimation sensors, which both sprayers are equipped with, ensuring an optimal balance between efficacy and conservation.

2.2 | Hardware Design Overview

The smart camera consisted of an RGB camera, an 8-mm C-mount lens, and an embedded NVIDIA Jetson TX2 GPU unit in a small IP67 enclosure. Two types of smart camera were used in our research: a NEON-201B-JT2-X with a 1.2 Mpix global shutter camera (1280 × 960 pixels) and a NEON-202B-JT2-X with a 1.9 Mpix global shutter camera (1600 × 1200 pixels). The size and industrial specifications of the two smart cameras make them ideal for installation on a tractor or trolley. The network connection with the DSS and GNSS was established with a RUTX11 router and puck 5 antenna. The router was programmed to use a wired connection or WIFI when available and switched to mobile data when needed. As a result, the detections were uploaded in real time if there was a mobile network available or uploaded at a later time when WIFI became available. Other key features were the GALILEO location system and online platform for remote support. An ARCDIS-110APRG 10" capacitive touchscreen was added to

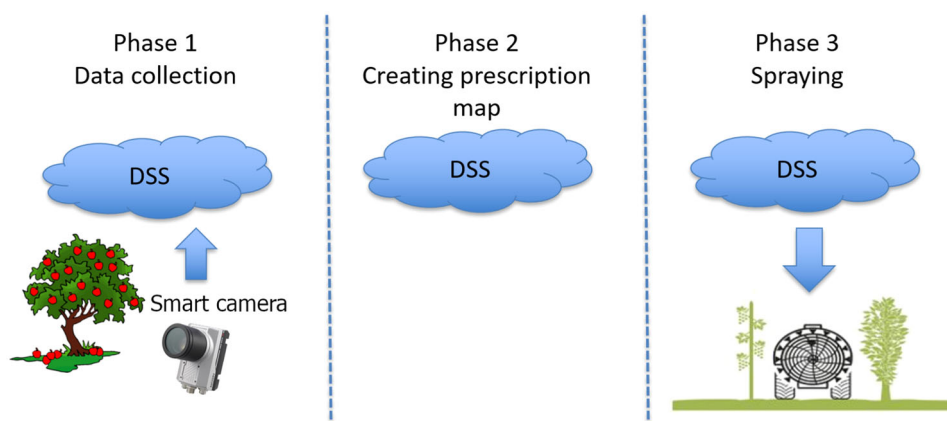


FIGURE 1 | General overview of the proposed system. [Color figure can be viewed at [wileyonlinelibrary.com](https://onlinelibrary.wiley.com/doi/10.1002/rfb.22510)]

control the system and give the operator visual feedback of the status. All internal connections were done through a HyperDrive HD-G218 USB-C HUB, with an 2TB Solid State Disk (SSD) to store the images for retraining of the deep learning models. The smart camera system consumed 42 W (12V/3.5A) without screen and 48 W (12 V/4 A) with screen. This meant that a car battery with 60Ah capacity could power the system for a full day. To protect against power surges of starting an engine a wide input 9–18VDC to 12VDC power converter and car charger was used to power the system. Figure 2 shows a schematic overview of the smart camera design, Figure 3 shows the components placed on a trolley that can be attached to a tractor, for real-time field measurements.

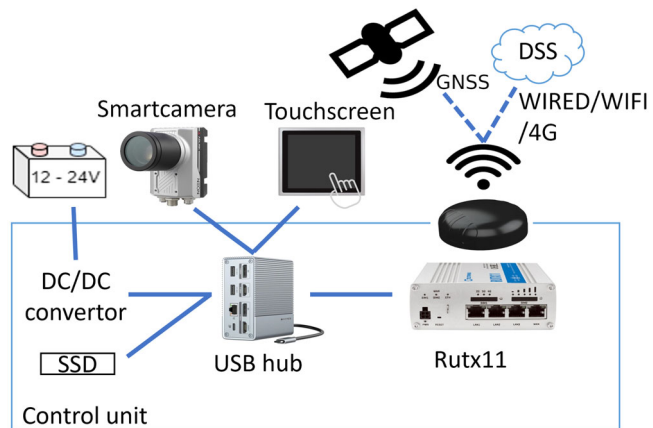


FIGURE 2 | Hardware overview, the USB hub in the center connects the smartcamera to all the peripherals: the SDD for storage, touchscreen for the user interaction and wireless connectivity and GNSS through the RUTX11. [Color figure can be viewed at [wileyonlinelibrary.com](https://onlinelibrary.wiley.com)]

2.3 | Software Design

The smart camera ran under the Linux operating system (Ubuntu 18.04 L4T with Jetpack 4.4 (R32.4.3)). The image acquisition and analysis software was activated by double-clicking a program icon on the main screen. Configuration was done with YAML config files (Oren, Clark, and Ingy 2021). The measurement protocol was that the smart camera scanned and processed the entire field in real time. To accomplish this, a multi-thread software architecture was used to speed the processing pipeline up as much as possible (Table 1). Multi-threading enabled to execute several threads at the same time, making optimal use of the CPU capacity of the smart camera. The software threads included image acquisition, image processing, storing GNSS locations and sending the system's output to the DSS. With this multi-threading, driving speeds of up to 5 km/h could be achieved.

The required time for the image analysis varied slightly from image to image. The image acquisition and storing of GNSS locations were executed at fixed intervals. The GNSS locations were stored in a ring buffer together with a timestamp. The location-timestamp fusions were used to compute the direction and speed of the trolley. With this information the current position was extrapolated to achieve more accurate localization between the GNSS pulses. Reliability of the GNSS coordinates was determined from the GNSS FIX parameter and the number of available satellites whose values were transferred by the GNSS receiver. The camera thread acquired images at a higher rate than the deep learning thread could process them. Therefore, a deque was used as buffer. The deep learning thread processed the images in a first in, last out fashion: this guaranteed that it always processed the most recent image. The deque had a fixed size and automatically removed the oldest image when it was full. For the analysis of the deep learning performance, it was important to save all results, therefore a

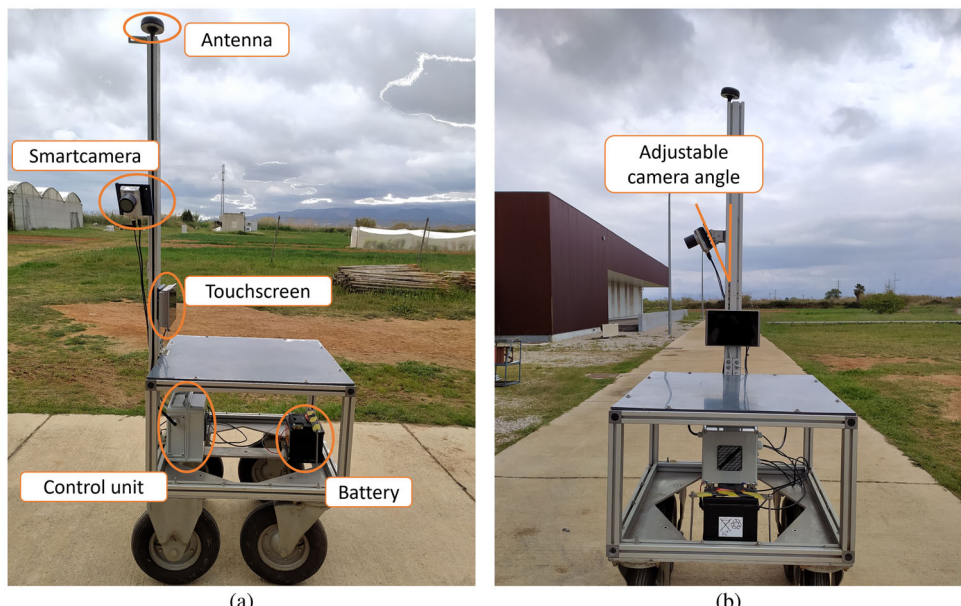
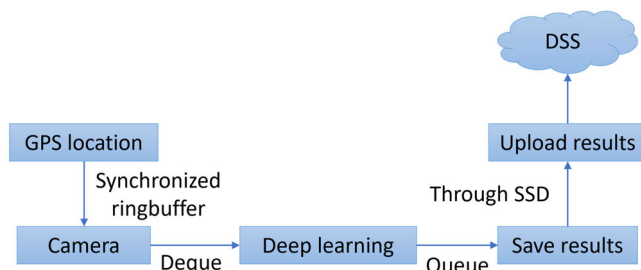


FIGURE 3 | The smart camera system deployed on a trolley that can be attached to a tractor. (a) Side view. (b) Front view. [Color figure can be viewed at [wileyonlinelibrary.com](https://onlinelibrary.wiley.com)]

TABLE 1 | Overview of software threads.

Thread	Task	Description
1	GNSS	Receive GNSS coordinates
2	Camera	Acquire images from camera
3	Decision	Run classification or detection model
4	Postprocessing	Group classification results and store the results on the SSD
5	Upload to DSS	This thread is activated once every 15 min to upload data to the DSS, batch uploads are used to lower the server load on the DSS

**FIGURE 4** | Overview of the software structure. [Color figure can be viewed at [wileyonlinelibrary.com](https://onlinelibrary.wiley.com)]

queue was used as buffer. The queue increased in size when new items were added and shrunk again when items were removed. At a configurable interval, all results and locations were transmitted to the DSS through an application programming interface (API).

Figure 4 shows a block diagram of the software structure. Figure 5 shows the screen of the smart camera system with the camera image, the disease detections and other useful information.

2.4 | Deep Learning

The three smart camera systems were equipped with an open-source object detection deep learning network, called You Only Look Once version 5 (YOLOv5) (Jocher 2020). Deep learning networks are currently evolving at a rapid pace. There are currently improved versions of YOLO available, but at the time our field experiments were conducted, YOLOv5 was the state-of-the-art network provided by Ultralytics, and therefore integrated on the smart camera. Object detection combines localization and classification of individual diseases in an image. We chose to use object detection instead of image classification because in real scenarios, an image may contain a mix of healthy and diseased regions or regions of multiple diseases. Image classification would struggle to provide detailed information when multiple diseases are present in an image, while object detection can handle such situations. Therefore, we considered object detection as a more scalable technique for future extension to other diseases within a crop.

YOLOv5, an extension of YOLO (Redmon et al. 2015), is a fast and robust one-staged object detection model that spatially separates bounding boxes and associated class probabilities. The entire detection pipeline is implemented as a single network

and can be optimized end-to-end directly based on the detection performance. An advantage is that YOLOv5 is less likely to predict false positives in the background, which our application takes great advantage of.

The YOLOv5 software was deployed in Python (version 3.6). For the deep learning functionalities, the Pytorch library was used (version 1.7.0), together with Torchvision (version 0.8.1). TensorRT (version 7.1.3.1) was used to further speed up the image analysis. With TensorRT, the average image analysis time was 0.45 s on both types of smart cameras (based on analyzing rescaled images of 640×640 pixels). The YOLOv5 object detection's were done in real time on the smart cameras. YOLOv5 was trained on images where the diseased leaves were annotated with an enclosing bounding box. The image annotation was performed by crop experts who used the open-source LabelImg program (Tzutalin 2020).

3 | Field Evaluation

3.1 | Field Campaign

Three smart camera systems were deployed in 2021 in Italy, Spain, and France. An commercial grape vineyard, apple orchard, and carrot field where used to ensure realistic field conditions. During the image acquisition there was no rain, but there was dew as the operators started to work in the early morning. The details of the field campaign can be found in Table 2 and Figures 6 and 7.

3.2 | Open-Set and Closed-Set Evaluation

From the acquired field images (Table 2), three smaller subsets of images were selected by the crop experts. These subsets were selected from the most diverse images of the total data set; hence, it is expected to be a good representation of a vast variety of field conditions. On these subsets, both the open-set and closed-set evaluations were performed. In the open-set evaluation, YOLOv5 was trained on images taken with different types of cameras in different cultivation conditions and different years (Figure 8a). In this evaluation scenario, the trained model was tested on images taken with the smart camera during the 2021 field campaign (Section 3.1). This type of evaluation enables us to test how a model trained on images taken under different conditions would perform when deployed on a smart camera. In the open-set evaluation, the transfer learning was executed with the network weights of a YOLOv5 network that was pretrained on the Microsoft COCO data set (Lin et al. 2014).



FIGURE 5 | Screen of the smart camera system during deployment. The purple-colored boxes are the disease detections from the deep learning model. [Color figure can be viewed at [wileyonlinelibrary.com](https://onlinelibrary.wiley.com/doi/10.1002/rob.22510)] [15564967, 0, Downloaded from https://onlinelibrary.wiley.com/doi/10.1002/rob.22510 by Wageningen University and Research Bhlthek, Wiley Online Library on [01/02/2025]. See the Terms and Conditions (https://onlinelibrary.wiley.com/terms-and-conditions) on Wiley Online Library for rules of use; OA articles are governed by the applicable Creative Commons License]

TABLE 2 | Details of the field campaign.

	Grape (Downy Mildew)	Apple (Apple Scab)	Carrot (<i>Alternaria</i>)
Location	Canelli (Italy)	Épila (Spain)	La Barp (France)
Acquisition days	14	5	3
Runtime (min)	1594	217	91
Smart camera	NEON-201B-JT2-X	NEON-202B-JT2-X	NEON-201B-JT2-X
Resolution (pixels)	1280 × 960	1600 × 1200	1280 × 960
Camera perspective	Side view	Side view	Top view
Distance to crop (m)	0.7	0.6	0.8
Field of view (m)	0.5 × 0.4	0.4 × 0.3	0.6 × 0.4
Images acquired	217,090	21,378	16,736



FIGURE 6 | Smart camera system deployed in an Italian grape vineyard for the detection of downy mildew. [Color figure can be viewed at [wileyonlinelibrary.com](https://onlinelibrary.wiley.com/doi/10.1002/rob.22510)] [15564967, 0, Downloaded from https://onlinelibrary.wiley.com/doi/10.1002/rob.22510 by Wageningen University and Research Bhlthek, Wiley Online Library on [01/02/2025]. See the Terms and Conditions (https://onlinelibrary.wiley.com/terms-and-conditions) on Wiley Online Library for rules of use; OA articles are governed by the applicable Creative Commons License]

In the closed-set evaluation, YOLOv5 was trained on images that were taken with the smart camera during the 2021 field campaign (Figure 8b). For equal comparison, the test images were the same as the test images used during the open-set



FIGURE 7 | Smart camera system deployed in a Spanish orchard for the detection of apple scab. [Color figure can be viewed at [wileyonlinelibrary.com](https://onlinelibrary.wiley.com/doi/10.1002/rob.22510)] [15564967, 0, Downloaded from https://onlinelibrary.wiley.com/doi/10.1002/rob.22510 by Wageningen University and Research Bhlthek, Wiley Online Library on [01/02/2025]. See the Terms and Conditions (https://onlinelibrary.wiley.com/terms-and-conditions) on Wiley Online Library for rules of use; OA articles are governed by the applicable Creative Commons License]

evaluation (refer to Figure 8a,b). For practical reasons, in the closed-set evaluation, the transfer learning was executed with the weights of the model that was trained in the open-set evaluation, which was initially pre-trained on the COCO data set. This pre-training method contributes to the generalization performance of the closed-set evaluation.

3.3 | YOLOv5 Training Details

YOLOv5 was trained on the images of the open-set and closed-set data set. The YOLOv5 training parameters were identical between the data sets. YOLOv5 was trained with three types of data augmentation to improve the generalization performance. The following default YOLOv5 augmentation techniques were used: color adjustments (random changes to the Hue, Saturation, and Value of the images), image flips (right, left, up, down) and image mosaicking (merge multiple images in 1 image). The training was done using RGB images that were resized to 640×640 pixels. This resolution was found to be the best compromise between detection performance and inference speed on the smart camera. YOLOv5 was trained with a batch size of 24 images for a maximum of 300 epochs. Because YOLOv5 is equipped with a software procedure that automatically saves the weights with the best performance on the validation data set, this software procedure guaranteed that the best-performing model weights were eventually used for model deployment.

3.4 | Evaluation Metrics

The evaluation metrics for the open-set and closed-set scenario, were calculated using thresholds on the YOLOv5 confidence level, the non-maximum suppression (NMS), and the Intersection over Union (IoU). The confidence level gives an impression of how confident YOLOv5 is in localizing and classifying the

object. NMS is a filtering technique to select the most appropriate bounding box from a group of overlapping bounding boxes. IoU is the evaluation metric for the overlap between the ground truth bounding box (B_{gt}) and the predicted bounding box (B_p), Equation 1. The IoU varies between zero (no overlap) and one (full overlap), and it highlights the classification and localization accuracy of the YOLOv5 model.

$$\text{IoU} = \frac{B_{gt} \cap B_p}{B_{gt} \cup B_p}. \quad (1)$$

For both open-set and closed-set evaluation, the thresholds for the IoU and NMS were, respectively, 0.5 and 0.3. The NMS threshold of 0.3 meant that YOLOv5 could output overlapping bounding boxes up to a maximum of 0.3 IoU. The confidence threshold values were obtained from the precision-recall curve of the individually trained YOLOv5 models. By inspecting the precision-recall curve, it was possible to choose the most appropriate confidence threshold by choosing the best point on the PR curve. This way we prevent too skewed behavior (either too many false positives or too many false negatives), and therefore evaluate the trained models in the best possible way on the test images of the smart camera. The used confidence thresholds are summarized in Table 3.

With the three thresholds, the total number of true positives (TP), false positives (FP), and false negatives (FN) were determined. A true positive (TP) is a diseased leaf that is detected as diseased leaf. A false positive (FP) is background that is detected as diseased leaf. A false negative (FN) is a diseased leaf that is not detected. With the total number of true positives, false positives, and false negatives, the precision (Equation 2) and recall (Equation 3) were calculated. The precision is the percentage of correct detections. The recall measures how well YOLOv5 can detect all diseased leaves. The harmonic mean between the precision and recall is expressed by the F1-score (Equation 4).

$$\text{Precision} = \frac{\text{TP}}{\text{TP} + \text{FP}}, \quad (2)$$

$$\text{Recall} = \frac{\text{TP}}{\text{TP} + \text{FN}}, \quad (3)$$

$$F1 - \text{score} = \frac{2 \cdot \text{Precision} \cdot \text{Recall}}{\text{Precision} + \text{Recall}}. \quad (4)$$

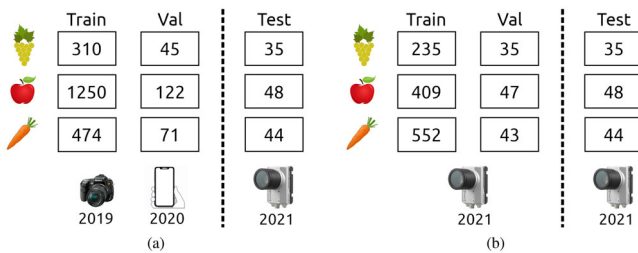


FIGURE 8 | (a) Open-set evaluation. (b) Closed-set evaluation. The numbers in the boxes represent the number of images. Note that the test images in the open-set and closed-set evaluation were the same. The corresponding image acquisition devices and years are expressed in the lower part of the figure. [Color figure can be viewed at [wileyonlinelibrary.com](https://onlinelibrary.wiley.com)]

TABLE 3 | YOLOv5 confidence thresholds that were used to obtain the evaluation metrics.

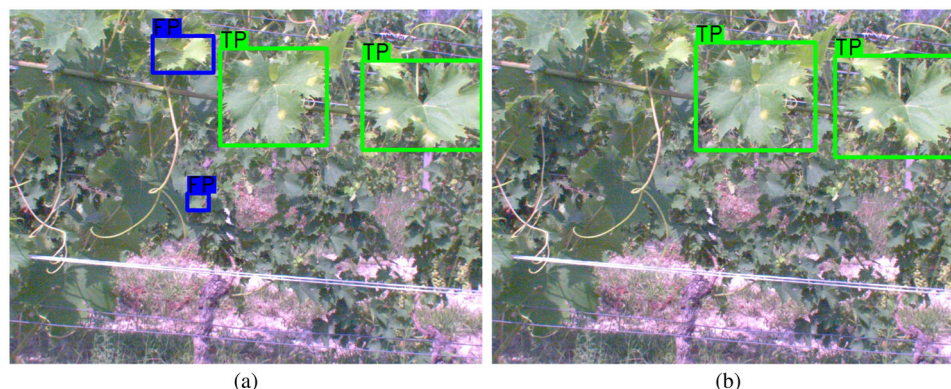
	Open-set evaluation	Closed-set evaluation
Grape (Downy Mildew)	0.5	0.4
Apple (Apple Scab)	0.05	0.3
Carrot (<i>Alternaria</i>)	0.4	0.4

4 | Results

The next three sections describe the performance for detecting downy mildew in grapes (Section 4.1), apple scab in apples (Section 4.2) and *Alternaria* leaf blight in carrots (Section 4.3) for the open-set and closed-set evaluation.

TABLE 4 | YOLOv5 performance for detecting downy mildew in grapes in the open-set and closed-set evaluation scenario.

Ground truth	Open-set evaluation			Closed-set evaluation		
	Downy mildew	Healthy	Recall	Downy mildew	Healthy	Recall
Downy mildew	47	58	44.8%	61	44	58.1%
Healthy	118	^a	^a	18	^a	^a
Precision	28.5%	^a	34.8% ^b	77.2%	^a	66.3% ^b

^aWith a one-class object detector, this comparison is not possible.^bF1-score.**FIGURE 9** | Object detection outputs of YOLOv5 on the same test image with two downy mildew infected leaves. (a) In the open-set evaluation, YOLOv5 detected both infected leaves, however it also produced two detections on healthy leaves (false positives). (b) In the closed-set evaluation, YOLOv5 detected both infected leaves, without false positives. TP and FP are abbreviations of respectively true positive and false positive. [Color figure can be viewed at [wileyonlinelibrary.com](https://onlinelibrary.wiley.com)]

4.1 | Downy Mildew Detection in Grapes

Table 4 summarizes the YOLOv5 performance for detecting downy mildew in grapes in the open-set and closed-set evaluation. In the open-set evaluation, the precision was 28.5% and the recall was 44.8%, resulting in an *F1*-score of 34.8%. In the closed-set evaluation, the *F1*-score increased to 66.3%. The biggest performance improvement was due to an increased precision score (77.2%), as the number of false positives decreased by 100 (18 instead of 118). The number of true positives increased from 47 to 61, resulting in a recall of 58.1%. Note that Table 4 lacks information on the true negative rate and negative predictive value, because YOLOv5 was trained as a one-class object detector for downy mildew (and not healthy). Figure 9 visualizes the performance difference between open-set and closed-set evaluation on the same test image from the smart camera.

4.2 | Apple Scab Detection in Apples

Table 5 summarizes the YOLOv5 performance for detecting apple scab in apples in the open-set and closed-set evaluation. In the open-set evaluation, the precision was 7.1% and the recall was 4.5%. The *F1*-score was 5.5%. This low performance was caused by a combination of leaf occlusion, different illumination conditions, motion blur, and the application of liquid copper sulfate onto the apple leaves to prevent the spread of the apple scab fungi (in the previous years, there was no application of copper sulfate). Copper sulfate caused the apple leaves to have a reflective coating and this caused more reflections of sunlight, a situation the open-set

detection model was not trained on. By retraining the model on these images in the closed-set evaluation, the *F1*-score considerably improved to 45.1%. Although this value is still suboptimal, it is probably closer to the maximum performance that could have been achieved given the complexity of the image scenes. In the closed-set evaluation, the precision was 45.5% and the recall was 44.8%. Figure 10 visualizes the performance difference between open-set and closed-set evaluation on the same test image from the smart camera.

4.3 | Alternaria Detection in Carrot

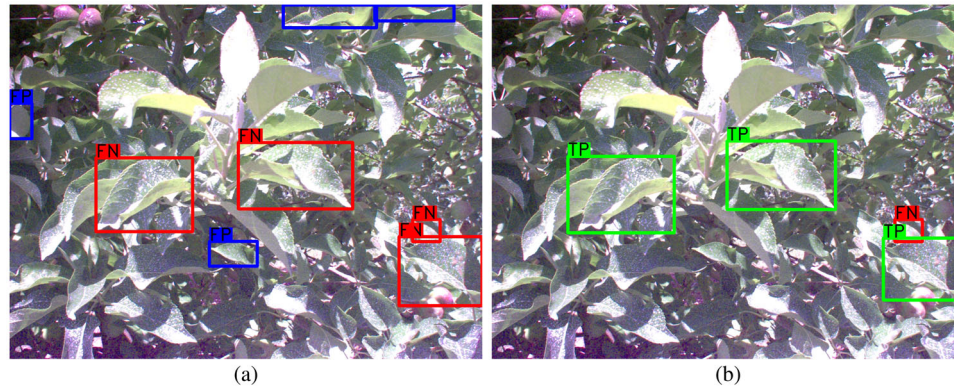
Table 6 summarizes the YOLOv5 performance for detecting *Alternaria* in carrot in the open-set and closed-set evaluation. In the open-set evaluation, the precision was 3.6% and the recall was 5.1%. The *F1*-score was 4.2%. The low performance was caused by the inability of the open-set model to detect the very tiny and subtle *Alternaria* lesions in the carrot leaves. Retraining on similar symptoms in the closed-set scenario, increased the *F1*-score to 42.1%. The precision was 47.9% and the recall was 37.6%. Figure 11 visualizes the performance difference between open-set and closed-set evaluation on the same test image from the smart camera.

5 | Data Set Differences

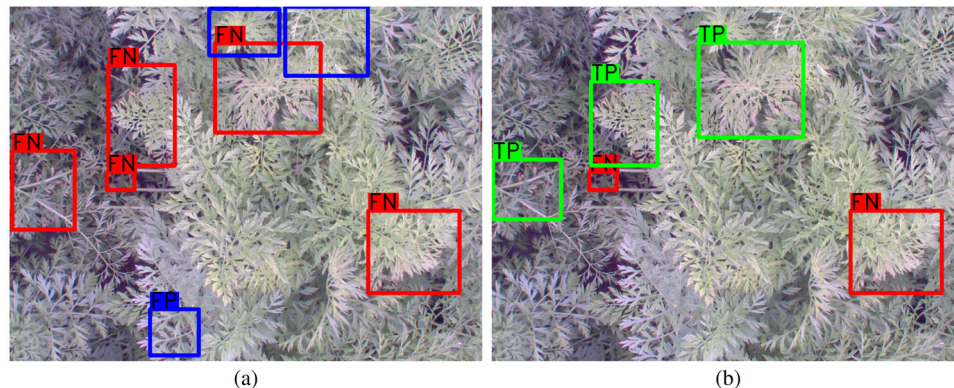
Given the poor performance of the open-set evaluation compared to the closed-set evaluation, we examined the differences between the data sets using Uniform Manifold Approximation and Projection (UMAP). UMAP (McInnes, Healy, and Melville 2020) is a nonlinear

TABLE 5 | YOLOv5 performance for detecting apple scab in apples in the open-set and closed-set evaluation scenario.

Ground truth	Open-set evaluation			Closed-set evaluation		
	Apple scab	Healthy	Recall	Apple scab	Healthy	Recall
Apple scab	6	128	4.5%	60	74	44.8%
Healthy	78	a	a	72	a	a
Precision	7.1%	a	5.5% ^b	45.5%	a	45.1% ^b

^aWith a one-class object detector, this comparison is not possible.^bF1-score.**FIGURE 10** | Object detection outputs of YOLOv5 on the same test image with four apple scab infected leaves. Due to the application of copper sulfate, there was a higher reflection of sunlight, making it harder to detect the apple scab. (a) In the open-set evaluation, YOLOv5 detected none of the infected leaves, and it produced four detections on healthy leaves (false positives). (b) In the closed-set evaluation, YOLOv5 detected three of the four infected leaves, without false positives. TP, FP, FN are abbreviations of respectively true positive, false positive, and false negative. [Color figure can be viewed at [wileyonlinelibrary.com](https://onlinelibrary.wiley.com)]**TABLE 6** | YOLOv5 performance for detecting *Alternaria* in carrot in the open-set and closed-set evaluation scenario.

Ground truth	Open-set evaluation			Closed-set evaluation		
	<i>Alternaria</i>	Healthy	Recall	<i>Alternaria</i>	Healthy	Recall
<i>Alternaria</i>	9	169	5.1%	67	111	37.6%
Healthy	238	a	a	73	a	a
Precision	3.6%	a	4.2% ^b	47.9%	a	42.1% ^b

^aWith a one-class object detector, this comparison is not possible.^bF1-score.**FIGURE 11** | Object detection outputs of YOLOv5 on the same test image with five *Alternaria* infected leaves. (a) In the open-set evaluation, YOLOv5 did not detect any of the infected leaves, and it also produced three detections on healthy leaves (false positives). (b) In the closed-set evaluation, YOLOv5 detected three of the five infected leaves. There were no false positives. TP, FP, FN are abbreviations of, respectively, true positive, false positive, and false negative. [Color figure can be viewed at [wileyonlinelibrary.com](https://onlinelibrary.wiley.com)]

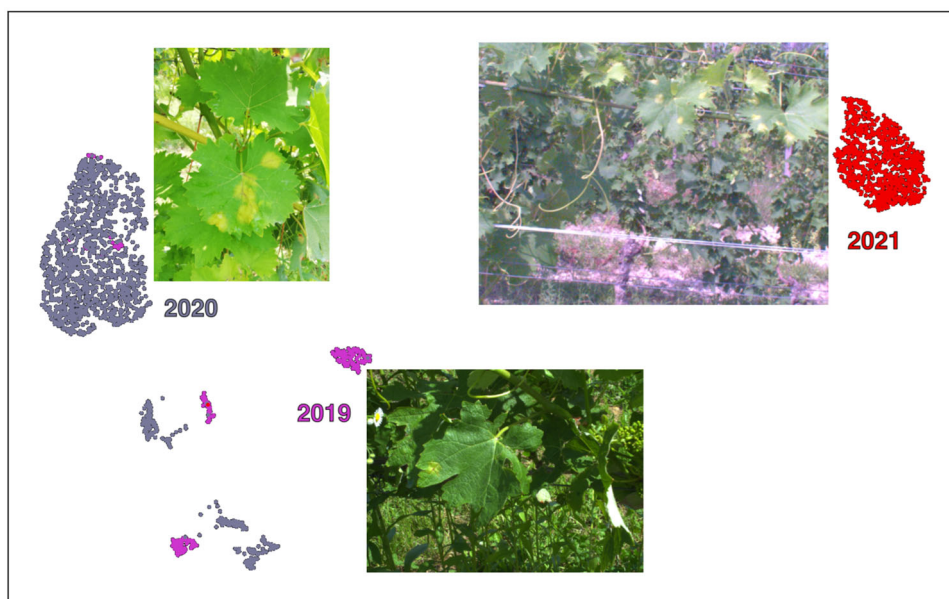


FIGURE 12 | UMAP image embedding visualization for the grape downy mildew data set. The colored points represent the image embeddings for each year. Purple = 2019 (open set), gray = 2020 (open set), red = 2021 (closed set). The images next to the clusters are example images from these data sets. [Color figure can be viewed at [wileyonlinelibrary.com](https://onlinelibrary.wiley.com/doi/10.1002/rob.22510)]

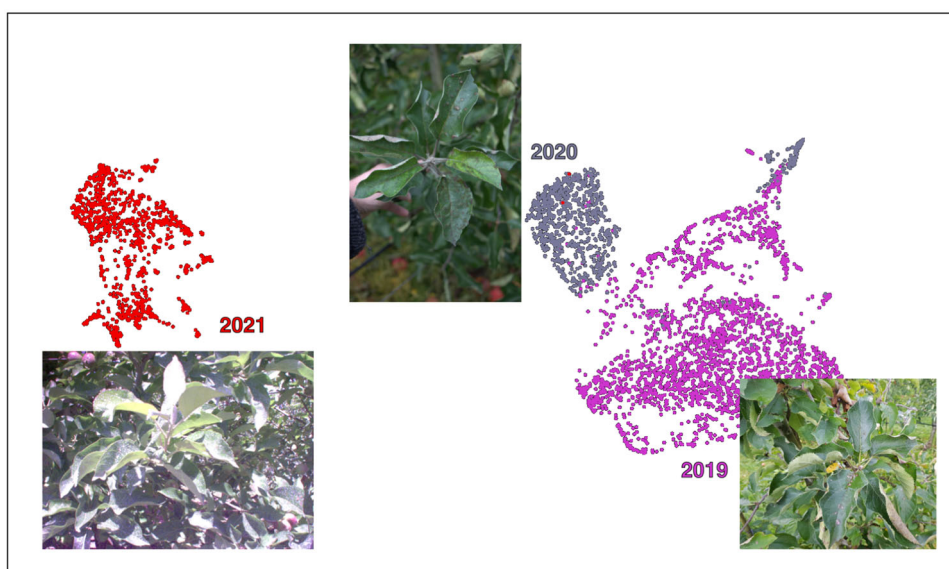


FIGURE 13 | UMAP image embedding visualization for the apple scab data set. The details of the clusters are similar as the ones from Figure 12. [Color figure can be viewed at [wileyonlinelibrary.com](https://onlinelibrary.wiley.com/doi/10.1002/rob.22510)]

dimensionality reduction technique that reveals complex patterns in high-dimensional data by constructing a graphical representation of the underlying data structures in lower dimensions. In these visualizations, clusters of data points that are closer together share common characteristics, unlike the more distant clusters. By applying UMAP to the three data sets, we can graphically visualize whether YOLOv5 might struggle with data from different data sets. This UMAP analysis implicitly explains why the open-set evaluation results are significantly worse than the closed-set evaluation results.

We used the FiftyOne software library to produce the UMAP visualization (FiftyOne 2023). Figures 12–14 visualize the data set differences for grape downy mildew, apple scab, and carrot

Alternaria, respectively. What is prominent in the three figures is that the open-set data sets (the purple- and gray-colored clusters) are considerably farther away in the UMAP than the closed-set data set (red-colored cluster). From the UMAP analysis, it is clear that the visual difference between the images of the open-set and closed-set data sets was notably (also considering the example images in Figures 12–14).

6 | Conclusions and Future Work

The fact that there were no hardware and software malfunctions during the combined 31-h test period, shows that the

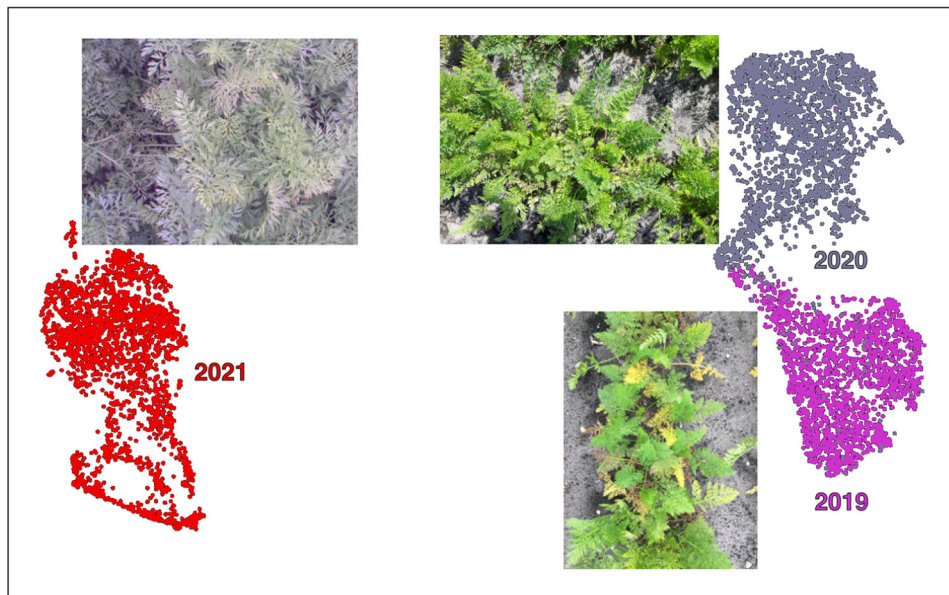


FIGURE 14 | UMAP image embedding visualization for the carrot *Alternaria* data set. The details of the clusters are similar as the ones from Figure 12. [Color figure can be viewed at [wileyonlinelibrary.com](https://onlinelibrary.wiley.com/doi/10.1002/rab.22510)] [wileyonlinelibrary.com](https://onlinelibrary.wiley.com/doi/10.1002/rab.22510)]

proposed smart camera system has the potential for robust disease detection in commercial vineyards, orchards, and fields. What this study also demonstrated is that testing in so-called open-set evaluation can produce worse results than testing in closed-set evaluation. A possible explanation is that the data sets were so different, because different cultivation methods and image acquisition methods were used. The primary differences in the images include variations in leaf color and size, infected region color and size, and background color and contrast. These differences are caused by the use of different cameras (cell phone vs. smart camera), the orientation of the camera due to various cultivation methods, the distance of the camera from the crop, and differing lighting conditions, such as sunlight from the front, top, or back. This observation was also clearly supported by our UMAP analysis.

Despite the poorer results, an open-set evaluation can give more realistic indications on how a deep learning model would perform when it was trained in conditioned circumstances and deployed in the field without retraining. This probably also applies to models trained on publicly available data sets such as PlantVillage. Although literature shows good performances on datasets like PlantVillage, implementation of the trained models in real field applications will certainly decrease the performance, due to changes in field conditions, where acquired images suffer from leaf occlusion, different illumination conditions and motion blur. In field conditions, shadows and highlights are caused by the position of the camera with respect to the sun which differs with the position of the crop and during the day. Also the color of the sunlight is different over the day and the season and depends on the weather conditions. The placement of our camera on a moving platform will lead to the occurrence of motion blur in cases where there is a disparity between the camera shutter speed and the speed of the platform. In summary, real field images usually differ considerable from images of conditioned data sets that often only contains images of detached leaves against a fixed background, acquired using

controlled illumination in the lab, something that was also clearly demonstrated by our UMAP analysis. Furthermore, care need to be taken when selecting a public data set for training, as these data sets can suffer from bias. For instance 49% accuracy was reached by training a machine learning model using only 8 pixels from the PlantVillage image backgrounds (Noyan 2022). Our study will hopefully encourage other researchers to also test their deep learning models in similar open-set evaluation scenarios for field application.

After retraining the model on the images from the smart camera, the performance notably improved. Especially for detecting downy mildew in grapes, the YOLOv5 performance in the closed-set scenario was promising. For detecting apple scab in apples and *Alternaria* leaf blight in carrot, the YOLOv5 performance was suboptimal, and this was mainly due to the reduced visibility of the disease symptoms due to the application of copper sulfate and because the disease symptoms were very subtle. Two practical considerations can make the application of even these suboptimal models feasible. First, false negative detections in one image frame can turn into true positive detections in the next image frame. Second, the resolution of the image analysis is much higher than the resolution of the final spray application. This implicitly means that the missed detections (false negatives) that are close to true positives, will be sprayed as well. Although, this approach is far more preferable than preventively spraying the entire orchard, future research should focus on evaluating the performance of the smart camera system as part of the IPM system.

A final note is that our smart camera system only used RGB color information. It has been demonstrated that the perception of diseased leaves in carrot and apple can be improved by using infrared information (Peller et al. 2021). Therefore, future research should investigate the use of multi-spectral cameras with channels in the infrared part of the spectrum for detecting the three diseases.

In a future field application, the smart camera system should also be equipped with a smart sampling method. Such a smart sampling method can automatically sample diverse images during model deployment about which the neural network is most uncertain. This can potentially allow for a faster network optimization in the open-set detection scenario (Blok et al. 2022).

Author Contributions

Gerrit Polder: conceptualization, methodology, supervision, project administration, writing—original draft preparation, writing—review and editing. **Pieter M. Blok:** methodology, software, data curation, investigation, writing—review and editing. **Tim van Daalen:** resources, software, writing—review and editing. **Joseph Peller:** resources, methodology, writing—review and editing. **Nikos Mylonas:** project administration, funding acquisition, writing—review and editing.

Acknowledgments

This paper is supported by European Union's Horizon 2020 research and innovation programme under grant agreement No 773718, project OPTIMA (Optimised Pest Integrated Management to precisely detect and control plant diseases in perennial crops and open-field vegetables). We would like to acknowledge the following people from Wageningen University and Research (WUR), the Agricultural University of Athens (AUA), University of Torino (UNITO), Universitat Politècnica de Catalunya (UPC), INRAE, and INVENIO for cooperation in the experiments and annotating of the images: Peter Frans de Jong (WUR), Dimitris Tsitsigiannis (AUA), Paolo Marucco (UNITO), Eric Mozzanini (UNITO), Emilio Gil (UPC), Paula Ortega (UPC), Fran Garcia (UPC), Jean-Paul Douzals (INRAE), and Laura Lescroart (INVENIO). We thank Roel Klein (WUR) for assistance with proofreading.

Data Availability Statement

A subset of the data that support the findings of this study are openly available in OPTIMA—RGB color images and multispectral images at <https://doi.org/10.5281/zenodo.6778647>, reference number 10.5281/zenodo.6778647.

References

- Agarwal, A., A. Sarkar, and A. K. Dubey. 2019. "Computer Vision-Based Fruit Disease Detection and Classification." In *Smart Innovations in Communication and Computational Sciences*, edited by S. Tiwari, M. C. Trivedi, K. K. Mishra, A. K. Misra, and K. K. Kumar, 105–115. Singapore: Springer.
- Ahmad, A., D. Saraswat, and A. ElGamal. 2023. "A Survey on Using Deep Learning Techniques for Plant Disease Diagnosis and Recommendations for Development of Appropriate Tools." *Smart Agricultural Technology* 3: 100083. <https://doi.org/10.1016/j.atech.2022.100083>.
- Amara, J., B. Bouaziz, and A. Algergawy. 2017. "A Deep Learning-Based Approach for Banana Leaf Diseases Classification." In *Datenbanksysteme für Business, Technologie und Web (BTW 2017)—Workshopband*, edited by B. Mitschang, D. Nicklas, F. Leymann, H. Schöning, M. Herschel, J. Teubner, T. Härder, O. Kopp, and M. Wieland, 79–88. Bonn: Gesellschaft für Informatik e.V.
- Ampatzidis, Y., A. Cruz, R. Pierro, et al. 2020. "Vision-Based System for Detecting Grapevine Yellow Diseases Using Artificial Intelligence." *Acta Horticulturae* 1279: 225–230. <https://doi.org/10.17660/ActaHortic.2020.1279.33>.
- Ash, G. 2000. "Downy Mildew of Grape." Plant Health Instructor. <https://doi.org/10.1094/PHI-I-2000-1112-01>.
- Ayaz, H., E. Rodríguez-Esparza, M. Ahmad, D. Oliva, M. Pérez-Cisneros, and R. Sarkar. 2021. "Classification of Apple Disease Based on Non-Linear Deep Features." *Applied Sciences* 11, no. 14: 6422. <https://doi.org/10.3390/app11146422>.
- Balafoutis, A., N. Mylonas, S. Fountas, et al. 2019. "Optima-Optimised Integrated Pest Management for Precise Detection and Control of Plant Diseases in Perennial Crops and Open-Field Vegetables." In *Conference Proceedings 12th EFITA-HAICTA-WCCA Congress*, 42–47.
- Bansal, P., R. Kumar, and S. Kumar. 2021. "Disease Detection in Apple Leaves Using Deep Convolutional Neural Network." *Agriculture* 11, no. 7: 6171. <https://doi.org/10.3390/agriculture11070617>.
- Blok, P. M., G. Kootstra, H. E. Elghor, B. Diallo, F. K. van Evert, and E. J. van Henten. 2022. "Active Learning With Maskal Reduces Annotation Effort for Training Mask R-CNN on a Broccoli Dataset With Visually Similar Classes." *Computers and Electronics in Agriculture* 197: 106917. <https://doi.org/10.1016/j.compag.2022.106917>.
- Chandler, D., A. S. Bailey, G. M. Tatchell, G. Davidson, J. Greaves, and W. P. Grant. 2011. "The Development, Regulation and Use of Biopesticides for Integrated Pest Management." *Philosophical Transactions of the Royal Society B: Biological Sciences* 366. <https://doi.org/10.1098/rstb.2010.0390>.
- Chen, Y., and Q. Wu. 2022. "Grape Leaf Disease Identification With Sparse Data via Generative Adversarial Networks and Convolutional Neural Networks." *Precision Agriculture* 24: 235–253. <https://doi.org/10.1007/s11119-022-09941-z>.
- Darshan, S. V. 2020. "Automated Diagnosis and Cataloguing of Foliar Disease in Apple Trees Using Ensemble of Deep Neural Networks." *International Research Journal of Engineering and Technology* 7, no. 5: 4230–4237.
- Dhaka, V. S., S. V. Meena, G. Rani, D. Sinwar, M. F. Kavita Ijaz, and M. Woźniak. 2021. "A Survey of Deep Convolutional Neural Networks Applied for Prediction of Plant Leaf Diseases." *Sensors* 21: 47491. <https://doi.org/10.3390/s21144749>.
- FiftyOne. 2023. *Using Image Embeddings*. https://docs.voxel51.com/tutorials/image_embeddings.html.
- Garcia, J., and A. Barbedo. 2013. *Digital Image Processing Techniques for Detecting, Quantifying and Classifying Plant Diseases*, Vol 2. <http://www.springerplus.com/content/2/1/660>.
- Grella, M., P. Marucco, I. Zwertvaegher, et al. 2022. "The Effect of Fan Setting, Air-Conveyor Orientation and Nozzle Configuration on Airblast Sprayer Efficiency: Insights Relevant to Trellised Vineyards." *Crop Protection* 155: 155. <https://doi.org/10.1016/j.cropro.2022.105921>.
- Hughes, D. P., and M. Salathe. 2015. *An Open Access Repository of Images on Plant Health to Enable the Development of Mobile Disease Diagnostics*.
- Jocher, G. 2020. <https://github.com/ultralytics/yolov5>.
- Kamilaris, A., and F. X. Prenafeta-Boldú. 2018. "Deep Learning in Agriculture: A Survey." *Computers and Electronics in Agriculture* 147: 70–90. <https://doi.org/10.1016/j.compag.2018.02.016>.
- Khan, M. A., T. Akram, M. Sharif, and T. Saba. 2020. "Fruits Diseases Classification: Exploiting a Hierarchical Framework for Deep Features Fusion and Selection." *Multimedia Tools and Applications* 79, no. 35: 25763–25783. <https://doi.org/10.1007/s11042-020-09244-3>.
- Kodors, S., G. Lacis, O. Sokolova, V. Zhukovs, I. Apeinans, and T. Bartulsons. 2021. "Apple Scab Detection Using CNN and Transfer Learning." *Agronomy Research* 19: 507–519. <https://doi.org/10.15159/AR.21.045>.
- Kole, D. K., A. Ghosh, and S. Mitra. 2014. "Detection of Downy Mildew Disease Present in the Grape Leaves Based on Fuzzy Set Theory." In *Smart Innovation, Systems and Technologies*. https://doi.org/10.1007/978-3-319-07353-8_44.

- Lamichhane, J. R., S. Dachbrodt-Saaydeh, P. Kudsk, and A. Messéan. 2016. "Toward a Reduced Reliance on Conventional Pesticides in European Agriculture." *Plant Disease* 100, no. 1: 10–24. <https://doi.org/10.1094/PDIS-05-15-0574-FE>.
- LeCun, Y., Y. Bengio, and G. Hinton. 2015. "Deep Learning." *Nature* 521, no. 7553: 436–444. <https://doi.org/10.1038/nature14539>.
- Li, P., R. Jing, and X. Shi. 2022. "Apple Disease Recognition Based on Convolutional Neural Networks With Modified Softmax." *Frontiers in Plant Science* 13. <https://doi.org/10.3389/fpls.2022.820146>.
- Lin, T.-Y., M. Maire, S. J. Belongie, et al. 2014. *Microsoft COCO: Common Objects in Context*. arXiv:1405.0312.
- Lindow, S. E. 1983. "Quantification of Foliar Plant Disease Symptoms by Microcomputer-Digitized Video Image Analysis." *Phytopathology* 73: 520. <https://doi.org/10.1094/Phyto-73-520>.
- Liu, B., Z. Ding, L. Tian, D. He, S. Li, and H. Wang. 2020. "Grape Leaf Disease Identification Using Improved Deep Convolutional Neural Networks." *Frontiers in Plant Science* 11: 1. <https://doi.org/10.3389/fpls.2020.01082>.
- Liu, B., Y. Zhang, D. He, and Y. Li. 2018. "Identification of Apple Leaf Diseases Based on Deep Convolutional Neural Networks." *Symmetry* 10, no. 1: 11.
- Mahlein, A.-K., M. Kuska, J. Behmann, G. Polder, and A. Walter. 2018. "Hyperspectral Sensors and Imaging Technologies in Phytopathology: State of the Art." *Annual Review of Phytopathology* 56: 535–558. <https://doi.org/10.1146/phyto.2018.56.issue-1>.
- McInnes, L., J. Healy, and J. Melville. 2020. *Umap: Uniform Manifold Approximation and Projection for Dimension Reduction*.
- Mishra, P., G. Polder, and N. Vilfan. 2020. "Close Range Spectral Imaging for Disease Detection in Plants Using Autonomous Platforms: A Review on Recent Studies." *Current Robotics Reports* 1, no. 2: 43–48. <https://doi.org/10.1007/s43154-020-00004-7>.
- Mohanty, S. P., D. P. Hughes, and M. Salathé. 2016. "Using Deep Learning for Image-Based Plant Disease Detection." *Frontiers in Plant Science* 7: 1. <https://doi.org/10.3389/fpls.2016.01419>.
- Natal-daLuz, T., T. Gevaert, C. Pereira, D. Alves, M. Arena, and J. P. Sousa. 2019. "Should Oral Exposure in Hypoaspis Aculeifer Tests Be Considered in Order to Keep Them in Tier I Test Battery for Ecological Risk Assessment of ppps?" *Environmental Pollution* 244: 871–876. <https://doi.org/10.1016/j.envpol.2018.10.113>.
- Noyan, M. A. 2022. *Uncovering Bias in the Plantvillage Dataset*. <https://doi.org/10.48550/arXiv.2206.04374>.
- Oerke, E.-C., H.-W. Dehne, F. Schönbeck, and A. Weber. 1994. *Crop Production and Crop Protection*. Amsterdam: Elsevier.
- Oren, B.-K., E. Clark, and d. N. Ingy. 2021. <https://yaml.org>.
- Peller, J. A., G. Polder, P. M. Blok, and I. Malounas. 2021. "Detecting Spectral Signals in Imaging for Disease Detection in Apple and Grape." In *Proceedings of the European Conference on Agricultural Engineering AgEng 2021*, edited by J. C. Barbosa, L. L. Silva, P. Lourenço, A. Sousa, J. R. Silva, V. F. Cruz, and F. Baptista, European Conference on Agricultural Engineering AgEng 2021, EurAgEng, Cranfield, 63–69.
- Polder, G., P. M. Blok, J. T. van Daalen, J. A. Peller, and N. Mylonas. 2021. "Early Disease Detection in Apple and Grape Using Deep Learning on a Smart-Camera." In *Proceedings of the European Conference on Agricultural Engineering AgEng 2021*, edited by J. C. Barbosa, L. L. Silva, P. Lourenço, A. Sousa, J. R. Silva, V. F. Cruz, and F. Baptista, European Conference on Agricultural Engineering AgEng 2021, EurAgEng, Cranfield, 51–56.
- Pradhan, P., B. Kumar, and S. Mohan. 2022. "Comparison of Various Deep Convolutional Neural Network Models to Discriminate Apple Leaf Diseases Using Transfer Learning." *Journal of Plant Diseases and Protection* 129: 1461–1473. <https://doi.org/10.1007/s41348-022-00660-1>.
- Redmon, J., S. K. Divvala, R. B. Girshick, and A. Farhadi. 2015. "You Only Look Once: Unified, Real-Time Object Detection." *CoRR, abs/1506.02640*. arXiv:1506.02640.
- Sandika, B., S. Avil, S. Sanat, and P. Srinivasu. 2016. "Random Forest Based Classification of Diseases in Grapes From Images Captured in Uncontrolled Environments." In *International Conference on Signal Processing Proceedings, ICSP, Chengdu, China, 1775–1780*. <https://doi.org/10.1109/ICSP.2016.7878133>.
- Singh, A., B. Ganapathysubramanian, A. K. Singh, and S. Sarkar. 2016. "Machine Learning for High-Throughput Stress Phenotyping in Plants." *Trends in Plant Science* 21: 110–124. <https://doi.org/10.1016/j.tplants.2015.10.015>.
- Singh, S., I. Gupta, S. Gupta, et al. 2022. "Deep Learning Based Automated Detection of Diseases From Apple Leaf Images." *Computers, Materials & Continua* 71, no. 1: 1849–1866.
- Subetha, T., R. Khilar, and M. S. Christo. 2021. "A Comparative Analysis on Plant Pathology Classification Using Deep Learning Architecture - Resnet and vgg19." *Materials Today: Proceedings*.
- Sünderhauf, N., O. Brock, W. Scheirer, et al. 2018. "The Limits and Potentials of Deep Learning for Robotics." *International Journal of Robotics Research* 37, no. 4–5: 405–420. <https://doi.org/10.1177/0278364918770733>.
- Thapa, R., K. Zhang, N. Snaveley, S. Belongie, and A. Khan. 2020. "The Plant Pathology Challenge 2020 Data Set to Classify Foliar Disease of Apples." *Applications in Plant Sciences* 8, no. 9: e11390. [10.1002/aps3.v8.9](https://doi.org/10.1002/aps3.v8.9).
- Too, E. C., L. Yujian, S. Njuki, and L. Yingchun. 2019. "A Comparative Study of Fine-Tuning Deep Learning Models for Plant Disease Identification." *Computers and Electronics in Agriculture* 161: 272–279. <https://doi.org/10.1016/j.compag.2018.03.032>.
- Tzutalin, D. 2020. <https://github.com/tzutalin/labelImg>.
- United Nations. 2015. *Population 2030 Demographic Challenges and Opportunities for Sustainable Development Planning*. <https://www.un.org/en/development/desa/population/publications/pdf/trends/Population2030.pdf>.
- Vaillancourt, L. J., and J. R. Hartman. 2000. "Apple Scab." *Plant Health Instructor*. <https://doi.org/10.1094/PHI-I-2000-1005-01>.
- Waghmare, H., R. Kokare, and Y. Dandawate. 2016. "Detection and Classification of Diseases of Grape Plant Using Opposite Colour Local Binary Pattern Feature and Machine Learning for Automated Decision Support System." In *3rd International Conference on Signal Processing and Integrated Networks. SPIN*. <https://doi.org/10.1109/SPIN.2016.7566749>.
- Wightwick, A. M., S. A. Salzman, G. R. S. M., Allinson, and N. W. Menzies. 2012. "Effects of Copper Fungicide Residues on the Microbial Function of Vineyard Soils." *Environmental Science and Pollution Research* 20: 1574–1585.
- Yan, Q., B. Yang, W. Wang, B. Wang, P. Chen, and J. Zhang. 2020. "Apple Leaf Diseases Recognition Based on an Improved Convolutional Neural Network." *Sensors* 20, no. 12: 3535. <https://doi.org/10.3390/s20123535>.
- Zhu, J., A. Wu, X. Wang, and H. Zhang. 2020. "Identification of Grape Diseases Using Image Analysis and bp Neural Networks." *Multimedia Tools and Applications* 79: 14539–14551. <https://doi.org/10.1007/s11042-018-7092-0>.
- Zwertvaegher, I., A. Lamare, J. Douzals, et al. 2022. "Boom Sprayer Optimizations for Bed-Grown Carrots at Different Growth Stages Based on Spray Distribution and Droplet Characteristics." *Pest Management Science* 78: 1729–1739.